Surface and Bulk Structure of Segmented Poly(ether urethanes) with Perfluoro Chain Extenders. 2. FTIR, DSC, and X-ray Photoelectron Spectroscopic Studies

Sung Chul Yoon and Buddy D. Ratner*

National ESCA and Surface Analysis Center for Biomedical Problems, Department of Chemical Engineering and Center for Bioengineering, BF-10, University of Washington, Seattle, Washington 98195. *Received February 18, 1987*

ABSTRACT: Segmented fluorine-containing poly(ether urethanes) were synthesized from 4,4′-methylenebis(phenylene isocyanate) (MDI) and poly(tetramethylene glycol) (PTMO) of molecular weight 2000 and chain extended with 2,2,3,3-tetrafluoro-1,4-butanediol or 2,2,3,3,4,4-hexafluoro-1,5-pentanediol. These polymers were studied by using Fourier transform infrared spectroscopy (FTIR), differential scanning calorimetry (DSC), and X-ray photoelectron spectroscopy (XPS). All FTIR and DSC results confirmed the bulk structural similarity between fluorinated and corresponding conventional polyurethanes. The XPS fluorine content data also correlated well with the FTIR and DSC results, suggesting that polyurethanes with good phase segregation concentrate the polyether component at their surface.

Introduction

Many studies utilizing X-ray photoelectron spectroscopy (XPS) to analyze the surfaces of block copolymers have been performed. Two goals have dominated this body of work: to clarify surface chemistry–biological response relationships of the materials[1–5] and to characterize compositional and morphological relationships.[6–11]

Careful scrutiny of experimental conditions must be exercised for results from such surface studies to be truly significant. Low molecular weight materials can dominate the surface and interfere with the elucidation of characteristic relationships.[11] This low molecular weight material can be removed by fractionation or extraction. Appropriate calibration spectra should be run to allow a more precise interpretation of XPS data. Finally, if the angular dependent XPS method is used, the sample surfaces must be verified as smooth.

In our previous XPS study of segmented poly(ether urethanes) and poly(ether urethane ureas), the above concerns were addressed and satisfied.[11] In that study, the hard-segment moiety was specifically labeled with fluorine atoms by using various perfluoro chain extenders. The fluorine labeling simplifies the analysis of the XPS spectra of polyurethanes in three ways: by reducing the dependency on the N_{1s} signal in the localization of the hard segment, by providing a signal of high intensity for the hard segment and by improving the ability to accurately resolve the C_{1s} spectrum. With these enhancements in the analysis of polyurethane spectra, the loci of hard segments at the surface can be traced more quantitatively and precisely.

In the previous report,[11] we found by using XPS that the 2,2,3,3,4,4-hexafluoro-1,5-pentanediol (FP) chain-extended polymers (with an odd number of carbons in the diol chain extender) have more hard segment at the surface than the even-diol, 2,2,3,3-tetrafluoro-1,4-butanediol (FB), polymers. Also, a decrease in the chain length of the soft segment induced an enrichment of hard segment at the surface. Thus, the variables which determine the bulk properties of multiblock copolymers, such as the type of chain extender (diamine or diol),[12–16] the number of carbons in linear low molecular weight chain extenders,[14–17] and the chain lengths of soft segments,[12,18,19] were assumed to affect the surface structural organization of fluorinated and nonfluorinated polyurethanes in a similar manner. A recent secondary ion mass spectrometry (SIMS) study[20] has corroborated the results described in ref 11.

The previous study attempted to relate the extent of soft-segment enrichment at the surface to the extent of phase separation in the bulk. However, bulk properties were not directly measured in that study. The primary goals of this study are (1) to substantiate the assumption of bulk structural similarities between polyurethanes prepared with fluorinated and nonfluorinated chain extenders by using Fourier transform infrared spectroscopy (FTIR) and differential scanning calorimetry (DSC) and (2) to further clarify the relationship between the bulk and surface structures of segmented polyurethanes.

Table I
Compositions of Fluorodiol Chain-Extended Segmented Polyurethanes

samples	molar ratio MDI/chain extender/PTMO	hard seg, wt %	feed chain extender, wt %
PEU-2000-FB-0	1:0:1	11.1	0
PEU-2000-FB-2	1.3:0.3:1	15.8	2.0
PEU-2000-FB-6	2:1:1	24.9	6.1
PEU-2000-FB-11	3:2:1	35.0	10.5
PEU-2000-FB-14	4:3:1	42.7	13.9
PEU-2000-FB-19	6:5:1	53.6	18.8
PEU-2000-FB-23	9:8:1	64.0	23.4
PEU-2000-FB-28	15:14:1	75.1	28.3
PEU-2000-FP-8	2:1:1	26.3	7.8
PEU-2000-FP-17	4:3:1	45.0	17.4
PEU-2000-FP-23	6:5:1	56.2	23.2

Experimental Section

Materials. Details of the preparation, purification, and characterization of the fluorine-labeled segmented poly(ether urethanes) based on methylenebis(phenylene isocyanate) (MDI) and poly(tetramethylene glycol) (PTMO) can be found in a previous paper.[11] All polymers were prepared by using the two-step solution polymerization technique outlined in Chart I. The composition data for the polymers under consideration in this study are shown in Table I; the chain extenders used were either tetrafluorobutanediol or hexafluoropentanediol. An example of the polymer nomenclature used is as follows: PEU-2000-FB-28 consists of a PTMO 2000-containing prepolymer unit and a tetrafluorobutanediol (FB) chain extender whose feed fraction was 28% by weight.

In the preparation of non-chain-extended or slightly chain-extended polymers, PEU-2000-FB-0, PEU-2000-FB-2 and PEU-2000-FB-6, toluene was used as a reaction solvent to obtain a high conversion and to increase the molecular weight.[21] The concentration of reactants was ~10% (w/v) or less.

* To whom correspondence should be addressed.

0024-9297/88/2221-2392$01.50/0

Chart I
Synthesis of Fluorine Diol Chain-Extended Poly(ether urethanes)

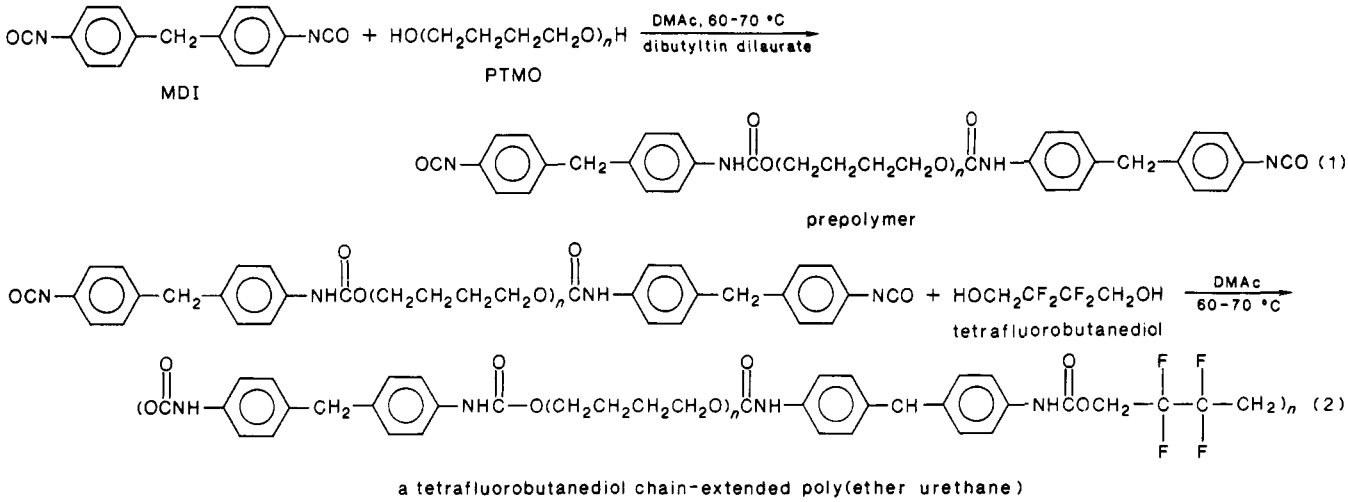

Polymer Characterization. A. Fourier Transform Infrared Spectroscopy (FTIR). For all polymers, *N,N*-dimethylacetamide (DMAc) was used as the casting solvent. Each sample for infrared analysis was prepared by casting a thin film onto a sodium chloride (NaCl) window from a 1% (w/v) solution in DMAc. The solvent was slowly evaporated under rough vacuum, and the sample was further dried under higher vacuum (0.1 Torr) at room temperature for 1 week to completely remove the solvent. Infrared spectra were acquired on an Analect FX-6200 Fourier transform infrared spectrometer in the high-resolution mode (resolution, 1.6 cm^{-1}). Fifty scans or more were averaged for each sample.

B. Differential Scanning Calorimetry (DSC). The Perkin-Elmer DSC-1B differential scanning calorimeter used for the thermal transition behavior study was calibrated with indium and *n*-octane. Experiments were carried out at a heating rate of 20 °C/min under a dry helium purge. The sample size was in the range of 10–15 mg. In this study, the midpoint of the glass transition process represented the glass transition temperature, and melting points referred to peak temperatures. The melting endotherm area was measured with a mechanical planimeter. The high-temperature (30–280 °C) DSC scan data were obtained on a Du Pont 9900 thermal analyzer.

The polymer samples were directly cast onto DSC pans from 20% (w/v) solutions in DMAc. The solvent was slowly evaporated in a laminar flow hood for 1 day. The specimens were subjected to further drying under vacuum at room temperature for 10 days.

C. X-ray Photoelectron Spectroscopy (XPS). A Surface Science Laboratories SSX-100 ESCA spectrometer was used to analyze all surfaces. An electron flood gun was used to neutralize surface charging. The quantitation of data and the sample mounting geometry for angular dependent studies are described in a previous paper.[11] Because of the low intensity of the N_{1s} signal from the samples, the number of scans was increased to 40–60 scans in the angular dependent experiments to increase the precision and accuracy of the nitrogen content data. In the angular dependent experiment with a small aperture (6° solid angle), 10–12 h were required to complete the data collection for each sample at five angles. During the experiment, no carbon contamination or sample degradation was observed.

The samples for the XPS study were prepared by centrifugally casting polymers onto clean glass disks from a 1% (w/v) solution in dry DMAc. All polymer samples used in the XPS study were purified by reprecipitating twice in methanol to remove low molecular weight materials that could potentially dominate the surface structure.[11]

Results and Discussion

A. Infrared Spectroscopy. In segmented polyurethane systems, the amide I band, which is principally due to carbonyl stretching vibration modes, has a relatively well-resolved absorption doublet.[22-24] The higher wavenumber peak (~1748 cm^{-1}) is associated with nonbonded C=O stretching absorption, and the lower wavenumber peak (~1720 cm^{-1}) represents the absorption of C=O hydrogen bonded with NH groups.

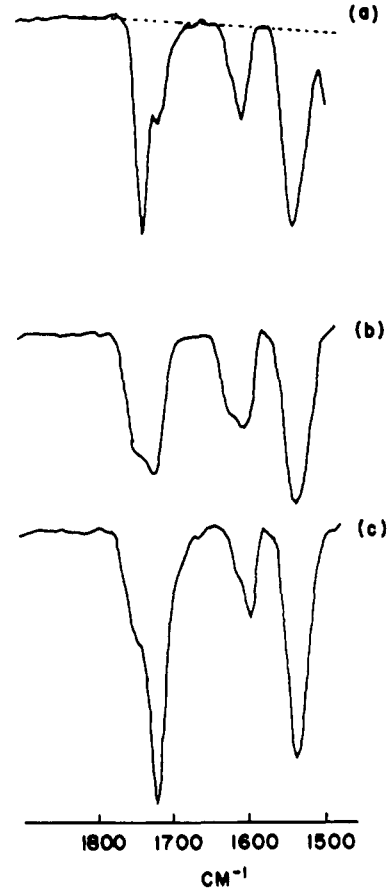

Figure 1. Infrared spectra of the amide I and II regions of (a) PEU-2000-FB-0, (b) polyurethane B cast from DMAc, and (c) polyurethane B cast from acetone.

The analysis of the FTIR spectra shown in Figure 1 makes use of the above general assignments for the C=O stretching absorption. A pure hard-segment polymer, poly[oxycarbonylamino-1,4-phenylenemethylene-1,4-phenyleneaminocarbonyloxy(2,2,3,3,4,4-hexafluoropentane-1,5-diyl)] (polyurethane B, see ref 11), shows different splitting of the C=O absorption band from two casting solvents, DMAc and acetone (Figure 1b,c). The peak shapes observed reflect the presence of an appreciable amount (ca. 50%) of free carbonyl in the polyurethane B

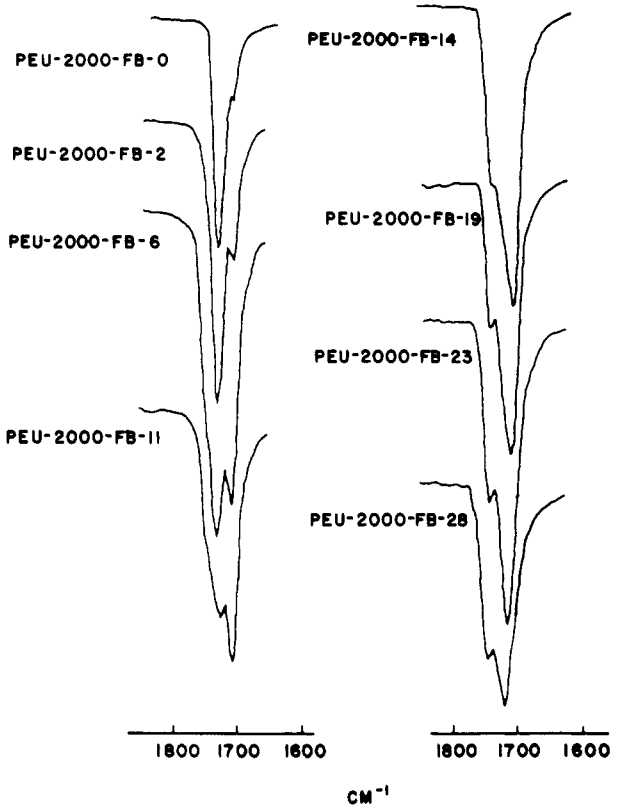

Figure 2. Infrared spectra of the PEU-2000-FB series polyurethanes in the C=O stretching region.

cast from DMAc (Figure 1b), while the same polymer cast from acetone exhibits little free carbonyl (Figure 1c). This difference between spectra implies that the nature and the degree of the molecular association of poly(ether urethanes) can be altered over a wide range and is sensitive to fabrication conditions.

The non-chain-extended polyurethane, PEU-2000-FB-0 cast from DMAc, also exhibits two bands in the carbonyl stretching region (Figure 1a). The strong peak at 1734 cm^{-1} reflects free carbonyls; the weak shoulder at 1714 cm^{-1} corresponds to hydrogen-bonded carbonyls. The assigned frequencies are comparable to reported values.[23,25] The full width at half-maximum (fwhm) of the free carbonyl peak is 20 cm^{-1}, slightly narrower than that of the hydrogen-bonded carbonyl peak whose value is 25 cm^{-1} for polyurethane B cast from acetone. The hydrogen-bonded and free carbonyl peak positions of polyurethane B are shifted to higher frequencies compared to those of PEU-2000-FB-0. This shift might be attributed to the matrix effect derived from the polarity difference between soft-segment-rich and hard-segment-rich matrices[26] and/or to the fluorine substitution effect in the diol chain extender, as seen previously in the XPS data. Thus, even though the carbamate carbon, —NH—C(=O)—O—CH_2—CF_2—, is removed by three bonds from the CF_2 group, the binding energy of the XPS carbamate C_{1s} core level is shifted by 0.5–0.8 eV more than was expected in the hydrocarbon analogue.[11] This may be indicative of a variation in the bond electron density of the carbonyl group that induces the infrared shift to higher frequencies.

The amide I band spectra for the PEU-2000-FB series polymers cast from DMAc are shown in Figure 2. As observed in the IR spectra of conventional polyurethanes,[18,24] an increase in hard-segment content corresponds to an increase in the relative intensity of hydrogen-bonded carbonyl bands. Upon careful examination of the carbonyl stretching band for PEU-2000-FB-6 and

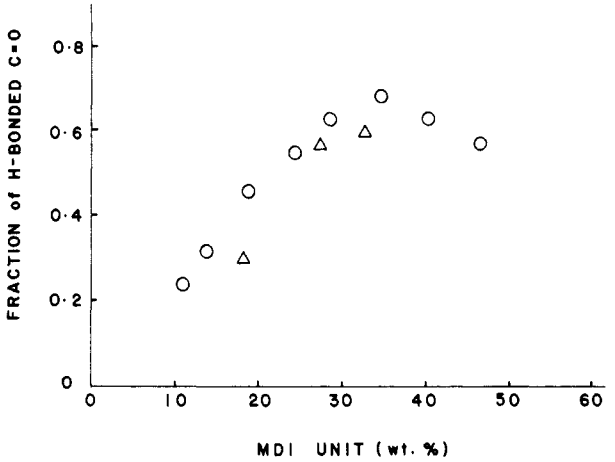

Figure 3. Dependence of the hydrogen-bonded carbonyl fraction on hard-segment content: (○) for the PEU-2000-FB series polymers and (△) for the PEU-2000-FP series polymers.

PEU-2000-FB-11, it is evident that there are at least three major components: the first slight hump at 1748 cm^{-1} is assigned to free carbonyls linked with the fluoro chain-extender units; the second peak at 1734 cm^{-1} reflects free carbonyls attached to soft-segment units; and the third at 1718 cm^{-1} represents hydrogen-bonded carbonyls. The third hydrogen-bonded carbonyl band actually consists of two overlapped contributions: the 1714 and 1720 cm^{-1} bands as assigned previously in the PEU-2000-FB-0 and polyurethane B spectra. For polymers with more than 43% hard segment by weight, only two distinct peak maxima were observed. PEU-2000-FB-28, which contains 75% hard segment by weight, has maximum absorption bands at 1719 and 1746 cm^{-1}. Therefore, the overall peak maxima of bonded and nonbonded carbonyl bands shift gradually toward the band maxima of polyurethane B with increasing hard-segment concentration. Polymers of the FP series showed a similar trend in the frequency shift and intensity variation of carbonyl stretching bands with changes in hard-segment content.

To accurately quantitate the molecular species from overlapped spectra, a deconvolution analysis utilizing exact line widths, peak positions, molar absorptivities, and strict forms of spectral distribution functions for the species is normally required.[23,27] However, because these carbonyl species exhibit (1) relatively well-separated peak maxima, (2) no significant difference in line width, and (3) extinction coefficients of free and bonded carbonyls similar to conventional polyurethane systems (where the ratio of the absorptivity of free and bonded carbonyls is 1),[18,23-25] the fraction of these species can be comparatively determined by the peak height method by assuming the same spectral distribution function. A flat baseline was chosen from 1800 to 1500 cm^{-1} as shown in Figure 1. The sample films cast from one drop (~20 μL) of 1% (w/v) polymer solutions were thin enough to be in a range where the Beer–Lambert law is obeyed.[27]

The fraction of hydrogen-bonded carbonyl calculated by the peak height method is plotted against MDI unit percent (by weight) in the polymers in Figure 3. The values were averaged over a minimum of two measurements and are reproducible within a maximum error of ±7%. Even with the simplified peak quantitation, the calculated results appear internally consistent. As the concentration of hard segment is increased in the polymer, the fraction of hydrogen-bonded carbonyls increases up to a limit. This concentration dependence is similar to the trend observed in conventional polyurethane systems.[25] The PEU-2000-FB series polymers have a higher fraction

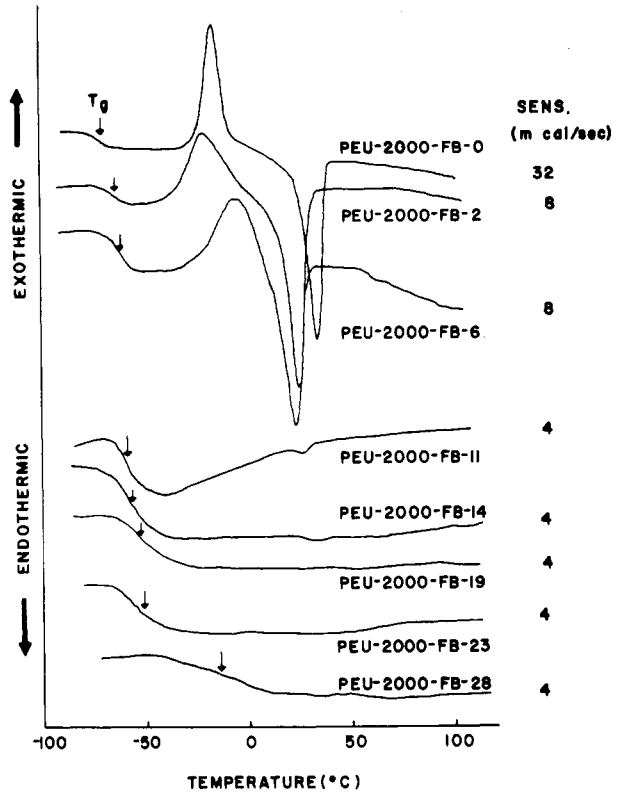

Figure 4. Low-temperature DSC thermograms for the as-cast PEU-2000-FB series polyurethanes: plots for FB-0, FB-2, FB-6, FB-11, FB-14, FB-19, FB-23, and FB-28.

of hydrogen-bonded carbonyls than the FP series of polymers with the same concentration of MDI units. If we assume that most of the hard segments in hard domains are hydrogen bonded,[18,25] we can explain this carbonyl difference in terms of the mixing behavior derived from the conformational energy difference in the chain-extender unit between the FB (even-diol) and FP (odd-diol) chain-extended polymers. The odd-diol polymers might be kinetically and thermodynamically less phase separated than the even-diol polymers and thus show a lower degree of hydrogen bonding. When fluorine atoms are substituted in the chain-extender region, this effect might become more pronounced because the fluorine substitution increases the conformational energy difference between the trans and gauche states.[28]

The soft-segment chain length effect on the extent of hydrogen bonding was also studied for the FB chain-extended polymers. An effect was anticipated because the configurational constraint produced by the reduction of chain length enhances the mixing of soft and hard segments.[29] However, for these FB chain-extended polymers, no detectable chain length effect on the hydrogen bonding was observed.

The maximum fraction of hydrogen-bonded carbonyl was found at 54% hard-segment content by weight for the PEU-2000-FB series polymers. This maximum suggests that a high hard-segment content induces the mixing of hard and soft segments, whereas a moderate increase in hard-segment content enhances microphase separation.

B. Differential Scanning Calorimetry. 1. Low-Temperature Thermograms. Figure 4 shows the low-temperature DSC thermograms of the as-cast PEU-2000-FB series samples. The polymers with low hard-segment content exhibited a melting endotherm characteristic of a crystalline PTMO phase. The non-chain-extended PEU-2000-FB-0 yielded the sharpest endotherm and recrystallization exotherm peaks. The area of the endotherm, normalized to the unit weight of the soft segment, decreases with increasing hard-segment concentration (Figure 5). The rapid disappearance of the melting endotherm indicates that the soft-segment crystallites are easily perturbed by an increased extent of hard- and soft-segment mixing and by a configurational constraint imposed through hard-domain formation.

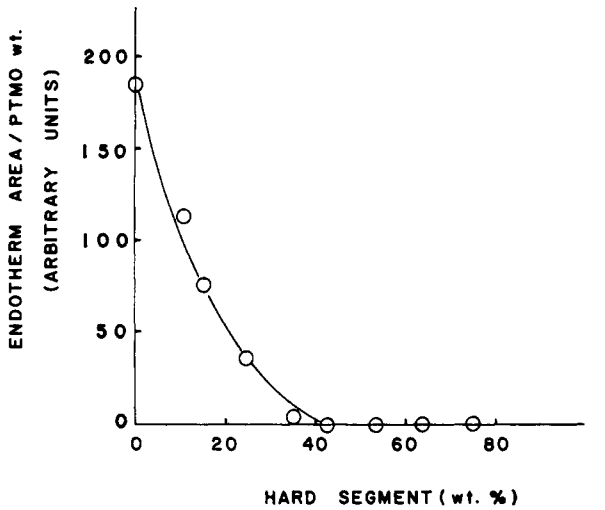

Figure 5. Dependence of the soft-segment melting endotherm area on the hard-segment content of the PEU-2000-FB series polyurethanes.

Table II
Thermal Transition Data

	T_g of soft seg, °C			T_m of soft seg, °C	T_m of hard seg, °C
	as-cast	2nd run	from Fox relatn		
pure soft segment				40	
PEU-2000-FB-0	−71	−69[a]	−68	32	
PEU-2000-FB-2	−68	−65	−64	24	
PEU-2000-FB-6	−63	−55	−54	23	
PEU-2000-FB-11	−58	−56	−42	25	231, 246
PEU-2000-FB-14	−56	−59	−32		234, 243
PEU-2000-FB-19	−54	−59	−16		239, 253
PEU-2000-FB-23	−46	−54	1.1		219, 237
PEU-2000-FB-28	−13	−16	22		234
PEU-2000-FP-8	−65				
PEU-2000-FP-17	−55	−52			
PEU-2000-FP-23	−37	−40			153
polyurethane A	84[b]				240
polyurethane B	88[b]				190, 215

[a] The data in the second column are for the second heating (20 °C/min) after cooling the melt at −20 °C/min in situ. [b] This is the T_g of the hard segment obtained from heating the quenched sample.

Melting point depression is a thermodynamic criterion for the miscibility of components in semicrystalline block copolymers or blends of pure component polymers.[30] The melting point depression for the soft-segment phase was observed with increased hard-segment concentration (Table II). The melt-cast pure PTMO 2000 had a sharp melting point of 40 °C. But the sample aged for several months shows two sharp melting points of 53 and 34 °C. The weak lower melting peak at 34 °C is due to metastable crystalline melting. Both the melting point drop and the high fraction of free carbonyls as shown in the FTIR data suggest significant mixing of soft and hard segments in the low-chain-extended polymers. Similarly, in the polymers containing high fractions of chain extender, particularly PEU-2000-FB-23 and perhaps PEU-2000-FB-28, the melting point depression of the hard-segment phase was also observed (Table II). This depression is also caused

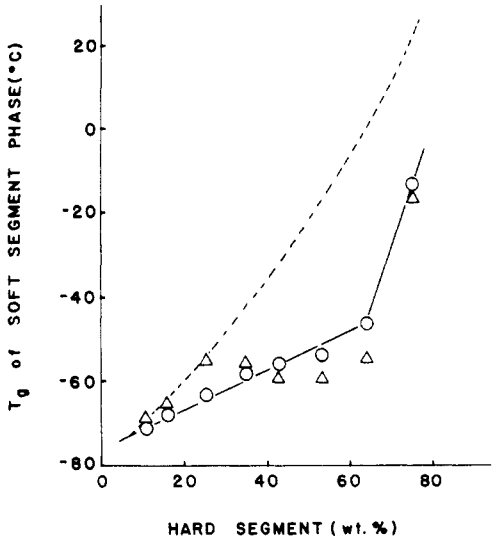

Figure 6. Effect of hard-segment content on the glass transition temperature (T_g) of the soft segment for the PEU-2000-FB series polyurethanes: (- - -) for the calculated T_g from the Fox relation; (○) for the T_g of the as-cast samples; (△) for the T_g of the samples in situ cooled at −20 °C/min.

by the increased solubilization of soft segments into hard domains as seen from the increased free carbonyl fraction at very high levels of hard-segment content.

Glass Transition Temperatures. The glass transition temperature (T_g) data (Table II) for the soft-segment phase suggest a trend in the degree of phase mixing over the whole composition range. As the hard-segment content and the chain length increase, the T_g of the soft segment for the as-cast samples increases, implying an increase in phase mixing. Figure 6 presents the T_g plotted as a function of the hard-segment content for the PEU-2000-FB series samples. The dotted curve denotes the calculated T_g by the Fox relation, $1/T_g = W_1/T_{g1} + W_2/T_{g2}$, where W_i is the weight fraction of component i in the soft microphase (i = 1, PTMO 2000; i = 2, hard segment) and T_{gi} is the glass transition temperature of the pure phase i. T_g is the expected overall glass transition temperature based on the complete mixing of the components.[29] For the present system, a T_g of 84 °C, which is the value determined from a hard-segment model polymer, fluorinated polyurethane A,[11] was used for the hard segment in the calculation. A T_g value of −79 °C was used for the PTMO 2000. To examine the thermal history effect on the glass transition, all original samples heated to the melting temperature of the hard segments were cooled to −100 °C at a cooling rate of −20 °C/min and reheated at the same heating rate of 20 °C/min as in the first run. The soft-microphase T_g data for samples subjected to such in situ thermal treatment are also shown in Figure 6 and Table II.

All of the as-cast and thermally treated samples exhibited soft-microphase glass transitions in a temperature range similar to that of the conventional MDI/butanediol (BD)/PTMO systems.[31,32] The thermal treatment raises the T_g of the soft-segment phase in the low hard-segment polymers, while the T_g behavior is reversed in the polymers containing more than 43% hard segment. In other words, during the heat treatment of as-cast polymers, the short hard segments of low hard-segment polymers can easily be mixed into the soft-segment phase, but polymers containing high concentrations of long hard segments remain phase separated. Thus, for high hard-segment polymers, the microphase separation is enhanced compared to the untreated as-cast samples. Specifically, the soft-microphase T_g of the thermally treated samples varies with hard-segment concentration in the same manner as in the melt-molded MDI/BD/PPO 2000 system[33] or the compression-molded MDI/BD/PTMO 2000 system.[31] The T_g initially increases up to PEU-2000-FB-6 and then remains relatively constant with increasing hard-segment content up to PEU-2000-FB-23. The T_g again increases abruptly to −16 °C at the 75% hard-segment polymer (PEU-2000-FB-28).

As shown in Figure 6, the observed T_g's of the three low hard-segment polymers, PEU-2000-FB-0, PEU-2000-FB-2, and PEU-2000-FB-6, are comparable to the calculated values, using the Fox relation for a completely mixed, disordered system. This agreement suggests that microphase separation might not occur in these three thermally treated polymers. It is also noticeable that the deviation of the experimental T_g from the value calculated by the Fox equation is largest for PEU-2000-FB-19 and PEU-2000-FB-23. The leveling of the experimental T_g in the intermediate polymers indicates that the soft-microphase compositions are relatively constant with increasing hard-segment content. This constant composition suggests that PEU-2000-FB-23 contains a total minimum amount of hard-segment materials dissolved within the soft-microphase domains so that the soft-microphase compositions are equivalent up to the 64% hard-segment polymer (PEU-2000-FB-23). On the basis of the soft-segment T_g data, it can be surmised that PEU-2000-FB-23 has the maximum degree of overall microphase separation within the bulk phase. In addition, this is supported by the small-angle X-ray scattering (SAXS) data for the MDI/BD/PPO 2000 system by Leung and Koberstein,[33] in which the results showed that the 60 wt % hard-segment polymer has a maximum overall degree of microphase separation.

In the case of the as-cast samples, the discontinuity in T_g behavior occurs for PEU-2000-FB-23 as shown in Figure 6. The discontinuity provides evidence for the morphological transition from discrete to continuous hard-microdomain structure in this range of hard-segment content and also implies the existence of a maximum in the overall degree of microphase separation. The composition at which the maximum degree of microphase separation appears is slightly different from the one at which the polymer has the maximum degree of hydrogen bonding as was shown in Figure 3. This discrepancy may be due to the fact that the IR data represent the overall molecular-level mixing, including the mixing of soft segments into the hard microdomains. The additional intraphase mixing was confirmed in the melting point depression of the hard segment for PEU-2000-FB-23 and PEU-2000-FB-28, as described previously.

The T_g values for the FP series, also listed in Table II, did not show any soft-segment crystallinity, except for PEU-2000-FP-8, as expected from the data for the conventional polyurethanes. Because the T_g (−80 °C) values were similar for the free PTMO 2000,[18,34] the T_g data can be used as a measure of phase mixing of the hard-segment units with the soft-segment phase in the PTMO 2000 polymer systems. For both FP and FB series of polymers, increasing the hard-segment content raises the soft-segment T_g; however, the concentration effect on the rise of T_g is more significant for the FP chain-extended polymers.

Phase-Segregation Dynamics. A sequence of in situ thermal cycles performed on the solvent-cast samples gives useful information on phase-segregation dynamics. In an MDI/ethylene diamine (ED)/PTMO poly(urethane urea) system, such heating (above the melting point) and cooling

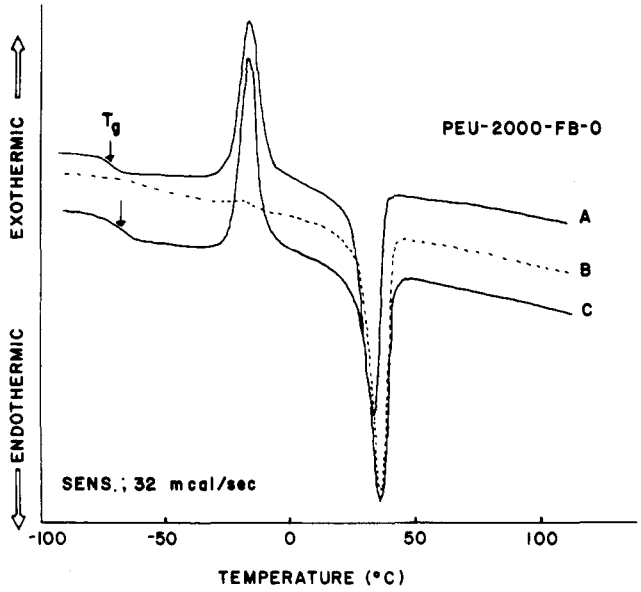

Figure 7. DSC curves of PEU-2000-FB-0: (a) first heating at 20 °C/min; (b) second heating at 20 °C/min after cooling at −5 °C/min from 150 °C; (c) third heating at 20 °C/min, after cooling at −20 °C/min.

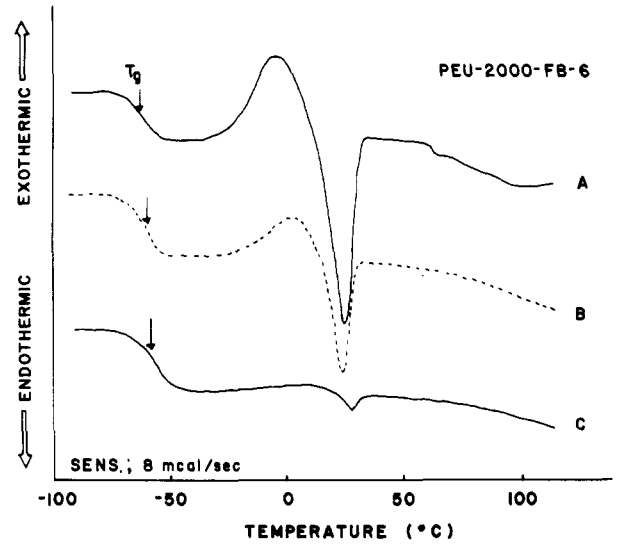

Figure 8. DSC curves of PEU-2000-FB-6: (a) first heating at 20 °C/min; (b) second heating at 20 °C/min after cooling at −5 °C/min from 150 °C; (c) third heating at 20 °C/min, after cooling at −20 °C/min.

increased the soft-segment crystallinity, even in a 25% hard-segment PTMO 2000 sample.[18] Slow cooling appeared to simultaneously enhance phase separation and soft-segment crystallization. Generally, the melt cycling process resulted in better phase separation of the poly(urethane ureas) than those initially prepared by solvent casting.

Since the polarity and the hydrogen-bonding capability of a diol chain-extended urethane unit are generally lower than those of a urea unit, thermal stabilization of phase structures and the extent of phase segregation are expected to be lower in the urethane. Figure 7 shows the heating DSC scans for PEU-2000-FB-0, which has no FB chain extender. After the first heating curve was obtained, the sample was cooled from 150 to −100 °C at −5 °C/min, then heated at 20 °C/min (the second heating), cooled again from 150 to −100 °C at −20 °C/min, and then heated again (the third heating). As expected for a polymer with only one MDI unit and a low concentration (11% by weight) of hard segment, only the thermal history associated with crystallization of the soft segment was observed. This well-separated, strong recrystallization peak from the soft segment appeared at −16 °C for the as-cast polymer. Although the slowly cooled sample did not exhibit the glass transition of the soft segment and the recrystallization exothermic peak, the faster cooling cycle (−20 °C/min) regenerated these characteristics. The measured melting endotherm area was constant—independent of the applied thermal treatment. This consistency in the endotherm area is another indication that no phase separation has occurred within the low hard-segment polymer matrix. The slightly chain-extended PEU-2000-FB-2 polymer exhibited a similar behavior (not shown), except that the recrystallization exothermic peak is twice as wide as that of the PEU-2000-FB-0 polymer.

Figure 8 shows the effect of the thermal history on the transitions of PEU-2000-FB-6, which has 25% hard segment by weight. It is noted that faster cooling (−20 °C/min) significantly reduced the extent of soft-segment crystallization and caused an increase in the soft-segment T_g from −63 to −55 °C. The same sample aged for 24 h at room temperature after quenching developed 67% of the melting endotherm area of the original as-cast sample. The same sample aged for 1 week at room temperature showed 100% recovery of the original soft-segment crystallinity and T_g. This means that the relaxation process toward the equilibrium structure was rather slow under room temperature annealing conditions. In poly(urethane ureas), a rapid recovery period during cooling was noted,[18] perhaps due to the higher polarity and hydrogen-bonding capability of the urea hard-segment component.

The diol chain-extended polyurethanes with a higher hard-segment concentration were far less sensitive to the applied thermal treatment in comparison with the corresponding poly(urethane ureas). For PEU-2000-FB-14 and PEU-2000-FB-19, thermal treatment of the as-cast samples induced a slight decrease in the soft-segment T_g (Figure 6), followed by a barely detectable enhancement or appearance of soft-segment crystallization (not shown), suggesting a slightly increased phase separation. This trend, along with the higher T_g's, gives additional evidence for the lower phase separation of the BD chain-extended polyurethanes compared with the ED chain-extended poly(urethane ureas).

2. High-Temperature Thermograms. High-temperature DSC measurements were made on the as-cast samples in order to characterize hard-segment melting. Figures 9 and 10 show high-temperature DSC thermograms of the FB chain-extended and FP chain-extended polyurethane samples, respectively. The melting thermograms for the hard-segment copolymers, polyurethane A (MDI/FB) and polyurethane B (MDI/FP), are also shown in Figure 9 and 10, respectively. A clean high-temperature melting endotherm was not observed for the polyurethanes containing 25% or less hard segment by weight. A similar observation has been made for conventional polyurethane systems.[25,33]

Some samples exhibited multiple melting endotherms as shown in Figure 9. The multiplicity of hard-segment melting endotherms strongly depends on the specimen preparation history such as casting condition, aging, annealing, and stretching.[32,35-37] For conventional, unoriented MDI/BD polyurethanes, wide-angle X-ray diffraction results[31,38] did not provide evidence for a highly crystalline phase with high symmetry. The hard-segment domains may, therefore, have a paracrystalline nature resulting from the wide sequence length distribution and the constraints imposed on chain packing by the linking of soft and hard

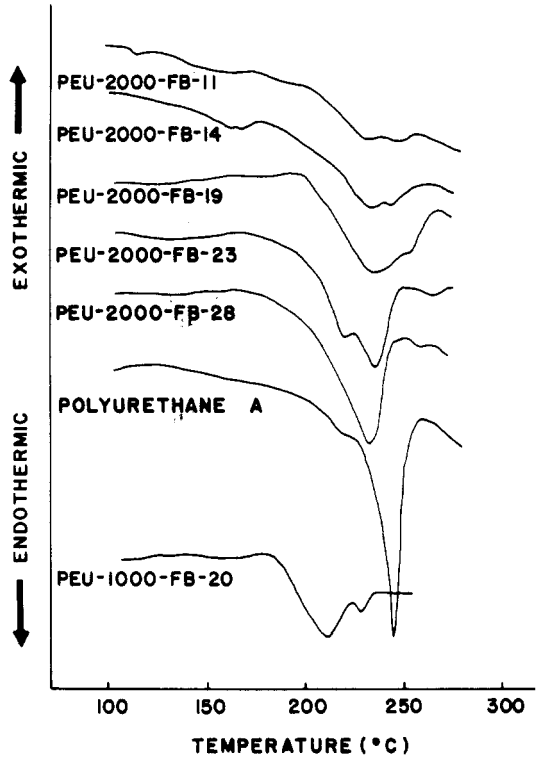

Figure 9. Hard-segment melting endotherms for the FB chain-extended polyurethanes and polyurethane A.

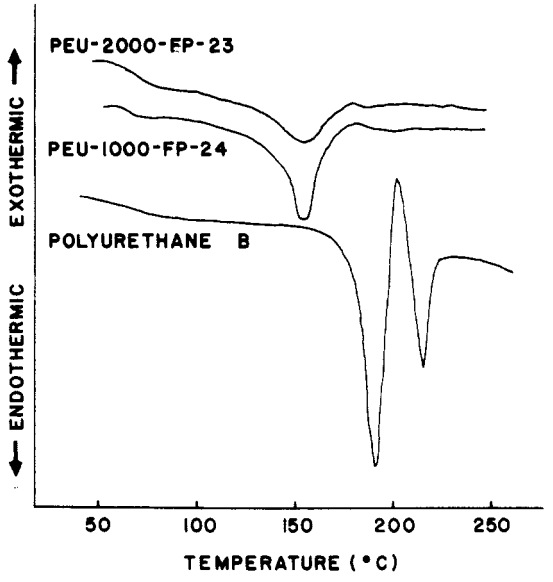

Figure 10. Hard-segment melting endotherms for the FP chain-extended polyurethanes and polyurethane A.

segments. Blackwell and Lee[36] ascribe at least some of the hard-segment melting endotherm peaks to polymorphism.

The hard-segment melting points (Table II and Figure 9) for the tetrafluorobutanediol chain-extended polymers are comparable to or higher than those for the conventional butanediol chain-extended copolymers.[25,32,33] The melting point (240 °C) of the as-precipitated MDI/FB copolymer (M_n = 26 000) is similar to that of a high molecular weight MDI/BD polymer (mp = 248 °C),[39] even with the substitution of fluorine atoms which have larger van der Waal's radii.

The as-precipitated MDI/FP copolymer (polyurethane B) exhibited melting endotherms at 190 and 215 °C (Figure 10). The strong lower temperature endotherm may be associated with the melting of metastable crystallites,

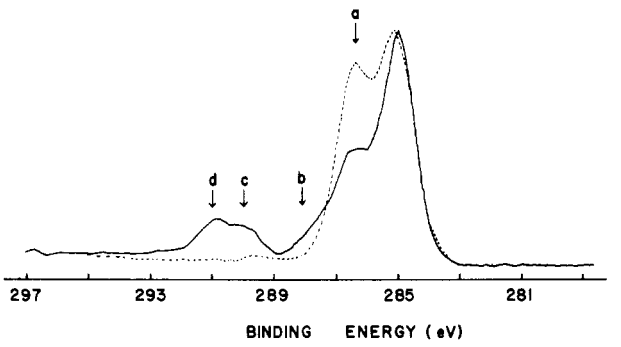

Figure 11. XPS C_{1s} core level spectra of PEU-2000-FB-2 (- - -) and PEU-2000-FB-28 (—).

whereas in polyurethane A, the endotherm appeared as a shoulder at ~210 °C. The significant melting point depression of polyurethane B by the additional CF_2 group might originate from the less effective intermolecular interaction in the odd-diol system. The weakened intermolecular interaction may cause the enhanced mixing of hard and soft segments. Consistent with this, the hard-segment melting point of the PEU-2000-FP-23 polymer is 40–60 °C lower than that of polyurethane B (Table II). However, in the FB chain-extended polymers, there is no significant difference in hard-segment melting points of segmented and pure hard-segment polymers.

All thermal analysis data presented here, along with the FTIR data discussed in the previous section, confirm similar trends in microphase separation behavior for the fluorinated and analogous nonfluorinated polyurethanes. Thus, the similar microphase separation behavior supports the conclusion of our previous paper, reiterated briefly in the Introduction, that the surface compositional organization of segmented polyurethanes or poly(urethane ureas) that are free of low molecular weight components can be correlated with the bulk structure of these polymers and with the extent of phase separation.

C. Surface Structure Characterization by XPS. In the previous study, we concluded that the relatively well phase-separated polymer, PEU-2000-FB-19, exhibits a significant compositional gradient between the surface and the bulk, in contrast to little or no difference in composition in the poorly phase-separated systems prepared with the FP chain-extender.[11] To investigate the surface compositional variation with hard-segment content, we carried out a systematic XPS analysis for the PEU-2000-FB series polymers. In Figure 11, the high-resolution (25 eV pass energy) C_{1s} XPS spectra are shown for the lowest and highest FB chain-extended polymers, PEU-2000-FB-2 and PEU-2000-FB-28, respectively. The maximum of the main peak at the lowest binding energy, associated with the unsubstituted hydrocarbon, was shifted to 285.0 eV for referencing the binding energy of other peaks. Detailed assignments of the binding energies corresponding to each of the chemical groups were made in the previous study.[11]

The increase in hard-segment content results in a decrease in the relative intensity of the first subpeak (designated (a) in Figure 11) at 286.4 eV. This subpeak is associated with the carbon singly bonded to oxygen originating from the soft segment of PTMO. An increase in the hard-segment content also results in an increase in the intensity of the second shoulder (b) at 287.8 eV, the third peak (c) at 290.1 eV, and the fourth peak (d) at 291.2 eV. These peaks reflect carbon singly bonded to oxygen in the chain-extender unit, the urethane carbonyl carbon, and the fluorine-substituted carbon, respectively. Thus, when the XPS analysis is performed with the photoemission detection normal to the sample surface, i.e., measuring 50–100

Table III
Surface and Bulk Compositions for the PEU-2000-FB Series Polymers

	F, atom %					N, atom %				
		surface					surface			
	bulk	0°	80°	80°/0°	80°/bulk	bulk	0°	80°	80°/0°	80°/bulk
PEU-2000-FB-2	0.25		0.25		1.00	1.43		1.01		0.77
PEU-2000-FB-6	1.41	0.82	0.89	1.08	0.63	2.02	1.78	1.03	0.58	0.51
PEU-2000-FB-11	2.37	1.41	1.02	0.72	0.43	2.28	2.08	1.21	0.58	0.53
PEU-2000-FB-14	4.30	2.80	1.76	0.63	0.41	2.71	2.87	1.58	0.55	0.58
PEU-2000-FB-19	4.56	3.48	1.97	0.57	0.43	3.70	3.08	2.02	0.66	0.54
PEU-2000-FB-23	7.03	7.37	5.67	0.77	0.81	4.22	4.62	3.77	0.82	0.89
PEU-2000-FB-28	8.89	9.66	9.12	0.94	1.03	4.66	5.19	4.83	0.93	1.04

Å into the sample, the intensity of each peak changes as expected with the variation in hard-segment concentration.

Data obtained by the angular dependent XPS method, indicative of the content of fluorine and nitrogen for the PEU-2000-FB series polymers as a function of depth into the surface, are presented in Table III. Throughout this section, the values for elemental composition are presented in terms of atom percent with respect to the four elements C, N, O, and F. The 80° take-off angle in Table III indicates sampling closest to the surface (i.e., ~10–20 Å). The bulk composition data for these polymers are also shown in Table III. Smaller values for the ratio 80°/bulk indicate steeper composition gradients between surface and bulk. Smaller values for the ratio 80°/0° indicate steeper compositional gradients in the outermost 50–100 Å. The consistently low ratios for the PEU-2000-FB-19 polymer indicate strong surface segregation in this highly phase-separated polymer.

In addition, the surface fluorine content of PEU-2000-FB-19 is less than the bulk value even at a 0° take-off angle (76% of the bulk value). For PEU-2000-FB-28, which consists of 75% hard segment, both the lack of an appreciable angular dependence of the XPS F_{1s} signal and the fact that the surface fluorine content is comparable to the bulk value suggest that the polymer has poor microphase separation. This observation is consistent with the FTIR and DSC analysis data. Data obtained based upon nitrogen content ratios and fluorine content ratios agree qualitatively. Both sets of data suggest that significant surface segregation is present for the FB-6, -11, -14, and -19 polymers.

The relationship between the bulk and the outermost surface composition (at θ = 80°) in PEU-2000-FB series polymers is illustrated in Figure 12. The diagonal line represents the equal composition at the surface and in the bulk, indicating no preferential enrichment at the surface and the random mixing of hard and soft segments. As shown in Figure 12, the fluorine content data reflect with greater sensitivity the phase-separation behavior in the bulk than do the nitrogen content data. The surface–bulk composition relation provides indirect evidence for the morphological transition[31,33,40] of the series of polymers from discrete to continuous hard domains. The maximum deviation in the surface composition from the diagonal composition line occurs for PEU-2000-FB-19 and PEU-2000-FB-14. Thus, the composition for the maximum phase separation as revealed by XPS analysis falls in a range similar to that determined by FTIR and DSC analysis.

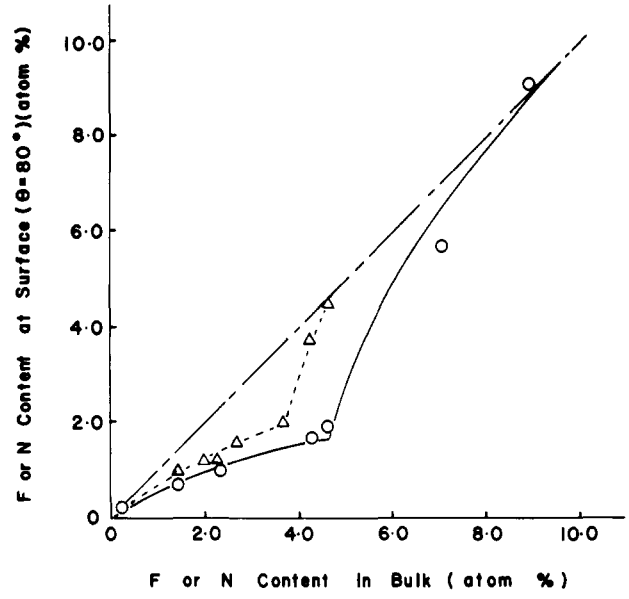

Figure 12. Effect of the bulk composition on the surface composition in the PEU-2000-FB series polyurethanes: (○) for fluorine content data; (△) for nitrogen content data.

Conclusions

MDI-based polyurethanes prepared with PTMO 2000, tetrafluorobutanediol, and/or hexafluoropentanediol were studied by FTIR and DSC to investigate the effects of the diol carbon number and the soft-segment chain length on the phase segregation behavior in the bulk. The overall trends related to phase mixing or phase separation of these fluorine-substituted polyurethanes were found to be similar to those of the corresponding conventional polyurethanes.

The IR analysis showed that the PEU-2000-FB series polymers have a higher ratio of hydrogen-bonded to nonbonded urethane carbonyls at the same level of hard-segment content than the FP series of polymers. The IR experiment also revealed that PEU-2000-FB-19, with 55% hard-segment content, has the maximum ratio of bonded to nonbonded urethane carbonyls, indicative of the overall maximum degree of microphase separation.

Conclusions based upon the DSC results are generally consistent with the IR results. For the PEU-2000-FB series polymers, a discontinuity in the T_g is observed at 65% hard-segment content. At very high levels of hard-segment content, the melting point depression of hard segment is observed. This depression suggests that a morphological transition from discrete to continuous hard domains occurs with increasing hard-segment content. Among the polymers with similar levels (55–60%) of hard segment, PEU-2000-FB-19 had the lowest T_g. These T_g results suggest that the even-diol chain-extended polymers with large soft-segment units are the most phase separated. The MDI/FB hard-segment polymer has a higher melting point than the MDI/FP polymer. The weakened intermolecular interaction is further evidence for the enhanced phase mixing of hard and soft segments in the FP chain-extended polyurethanes. In addition, the hard-segment melting point of the FB chain-extended polymers is almost identical with that of the nonfluorinated polyurethanes. This similarity implies that the partial symmetric fluorination

of the chain-extender unit has little effect on the intermolecular interactions between hard segments. Thus, all FTIR and DSC data substantiate the assumption in the previous XPS study that a structural analogy exists between the fluorinated and conventional polyurethanes.

Seven PEU-2000-FB polymers were systematically studied by using XPS to investigate the effects of bulk composition and hard block length on the surface and bulk structures for the relatively well phase-segregated system. It was found that the surface composition and fluorine depth profile data correlate well with the IR and DSC results and show a gradual morphological transition with hard-segment content. According to this result, the intermediate 2000-FB polymer with ~50% hard segment (FB-19) is the most phase separated of all the polymers studied here. The interrelationship between the FTIR, DSC, and XPS results leads to the conclusions that increased H-bonding generates more bulk-phase separation and that more bulk-phase separation leads to more surface-phase separation. Thus, the surface structure may be driven by the bulk structure.

Finally, throughout the XPS study of the polymers, no evidence of lateral inhomogeneity in surface composition was detected. Since the domain size of this multiblock copolymer system is much smaller (50–100 Å) than the X-ray spot size (minimum of 100 μm), a lateral or line scan across the surface cannot be used to learn about surface phase segregation. However, we can substantiate the absence of such surface-lateral domains from the angular dependent XPS experiment on highly phase-separated polymers.

Acknowledgment. Support from N.I.H. grants HL25951 and RR01296 has made these studies possible. Access to the Du Pont 9900 Thermal Analyzer was generously provided by Prof. J. C. Seferis. The editorial assistance of N. B. Mateo in the preparation of this manuscript is appreciated.

Registry No. (FP)(MDI)(PTMO) (block copolymer), 112666-67-8; (FB)(MDI)(PTMO) (block copolymer), 112666-66-7.

References and Notes

(1) Hanson, S. R.; Harker, L. A.; Ratner, B. D.; Hoffman, A. S. *J. Lab. Clin. Med.* **1980**, *95*, 289.
(2) Sa da Costa, V.; Brier-Russell, D.; Salzman, E. W.; Merrill, E. W. *J. Colloid Interface Sci.* **1981**, *80*, 445.
(3) Lelah, M. D.; Lambrecht, L. K.; Young, B. R.; Cooper, S. L. *J. Biomed. Mat. Res.* **1983**, *17*, 1.
(4) Lelah, M. D.; Pierce, J. A.; Lambrecht, L. K.; Cooper, S. L. *J. Colloid Interface Sci.* **1985**, *104*, 422.
(5) Takahara, A.; Tashita, J.; Kajiyama, T.; Takayanagi, M.; MacKnight, W. J. *Polymer* **1985**, *26*, 978.
(6) Thomas, H. R.; O'Malley, J. J. *Macromolecules* **1978**, *12*, 323.
(7) O'Malley, J. J.; Thomas, H. R.; Lee, G. M. *Macromolecules* **1979**, *12*, 996.
(8) Sha'aban, A. K.; McCartney, S.; Patel, N.; Yilgor, I.; Riffle, J. S.; Dwight, D. W.; McGrath, J. E. *Polym. Prepr. (Am. Chem. Soc., Div. Polym. Chem.)* **1983**, *24* (2), 130.
(9) Schmitt, R. L.; Gardella, J. A., Jr.; Magill, J. H.; Salveti, L., Jr.; Chin, R. L. *Macromolecules* **1985**, *18*, 2675.
(10) Schmitt, R. L.; Gardella, J. A., Jr.; Salveti, L., Jr. *Macromolecules* **1986**, *19*, 648.
(11) Yoon, S. C.; Ratner, B. D. *Macromolecules* **1986**, *19*, 1068.
(12) Paik Sung, C. S.; Hu, C. B.; Wu, C. S. *Macromolecules* **1980**, *13*, 111.
(13) Paik Sung, C. S.; Smith, T. W.; Sung, N. H. *Macromolecules* **1980**, *13*, 117.
(14) Bonart, R.; Morbitzer, L.; Muller, E. H. *J. Macromol. Sci. Phys.* **1974**, *89*, 447.
(15) Bonart, R. *Angew. Makromol. Chem.* **1977**, *58/59*, 259.
(16) Blackwell; J., Nagarajan, M. R.; Hoitink, T. B. *Polymer* **1982**, *23*, 950.
(17) Blackwell, J.; Quay, J. R.; Nagarajan, M. R.; Born, L.; Hespe, H. *J. Polym. Sci., Polym. Phys. Ed.* **1984**, *22*, 1247.
(18) Wang, C. B.; Copper, S. L. *Macromolecules* **1983**, *16*, 775.
(19) Wilkes, G. L.; Abouzahr, S. *Macromolecules* **1981**, *14*, 456.
(20) Hearn, M. J.; Briggs, D.; Yoon, S. C.; Ratner, B. D. *Surf. Interface Anal.*, **1987**, *10*, 384–391.
(21) Saunders, J. H.; Frisch, K. C. *Polyurethanes: Chemistry and Technology. Part* 1. *Chemistry*; Interscience: New York, 1962.
(22) Paik Sung, C. S.; Schneider, N. S. *Macromolecules* **1975**, *8*, 68.
(23) Srichatrapimuk, V. W.; Cooper, S. L. *J. Macromol. Sci. Phys.* **1978**, *815*, 267.
(24) Senich, G. A., MacKnight, W. J. *Macromolecules* **1980**, *13*, 106.
(25) Miller, J. A.; Lin, S. B.; Hwang, K. K. S.; Wu, K. S.; Gibson, P. E.; Cooper, S. L. *Macromolecules* **1985**, *18*, 32.
(26) Schrems, O.; Oberhoffer, H. M.; Luck, W. A. P. *J. Phys. Chem.* **1984**, *88*, 4335.
(27) Skrovanek, D. J.; Howe, S. E.; Painter, P. C.; Coleman, M. M. *Macromolecules* **1985**, *18*, 1676.
(28) Flory, P. J. *Statistical Mechanics of Chain Molecules*; Interscience: New York, 1969.
(29) Olabisi, O.; Robeson, L. M.; Shaw, M. T. *Polymer–Polymer Miscibility*; Academic: New York, 1979.
(30) Nishi, T.; Wang, T. T. *Macromolecules* **1975**, *8*, 909.
(31) Abouzahr, S.; Wilkes, G. L.; Ophir, Z. *Polymer* **1982**, *23*, 1077.
(32) Van Bogart, J. W. C.; Bluemke, D. A.; Cooper, S. L. *Polymer* **1981**, *22*, 1428.
(33) Leung, L. M.; Koberstein, J. T. *J. Polym. Sci., Polym. Phys. Ed.* **1985**, *23*, 1883.
(34) Hu, C. B.; Ward, R. S., Jr.; Schneider, N. S. *J. Appl. Polym. Sci.* **1982**, *27*, 2167.
(35) Leung, L. M.; Koberstein, J. T. *Macromolecules* **1986**, *19*, 706.
(36) Blackwell, J.; Lee, C. D. *J. Polym. Sci., Polym. Phys. Ed.* **1984**, *22*, 759.
(37) Briber, R. M.; Thomas, E. L. *J. Polym. Sci., Polym. Phys. Ed.* **1985**, *23*, 1915.
(38) Crystal, R. G.; Erhardt, P. F.; O'Malley, J. J. In *Block Copolymers*; Aggarwal, S. L., Ed.; Plenum: New York, 1970, pp 179–193.
(39) Qin, Z. Y.; Macosko, C. W.; Wellinghoff, S. T. *Macromolecules* **1985**, *18*, 553.
(40) Zdrahala, R. J.; Gerkin, R. M.; Hager, S. L.; Critchfield, F. E. *J. Appl. Polym. Sci.* **1979**, *24*, 2041.